DeepVoxels: Learning Persistent 3D Feature Embeddings
— Supplemental Document —

Vincent Sitzmann[1], Justus Thies[2], Felix Heide[3],
Matthias Nießner[2], Gordon Wetzstein[1], Michael Zollhöfer[1]
[1]Stanford University, [2]Technical University of Munich, [3]Princeton University

1. DeepVoxels Submodule Architectures

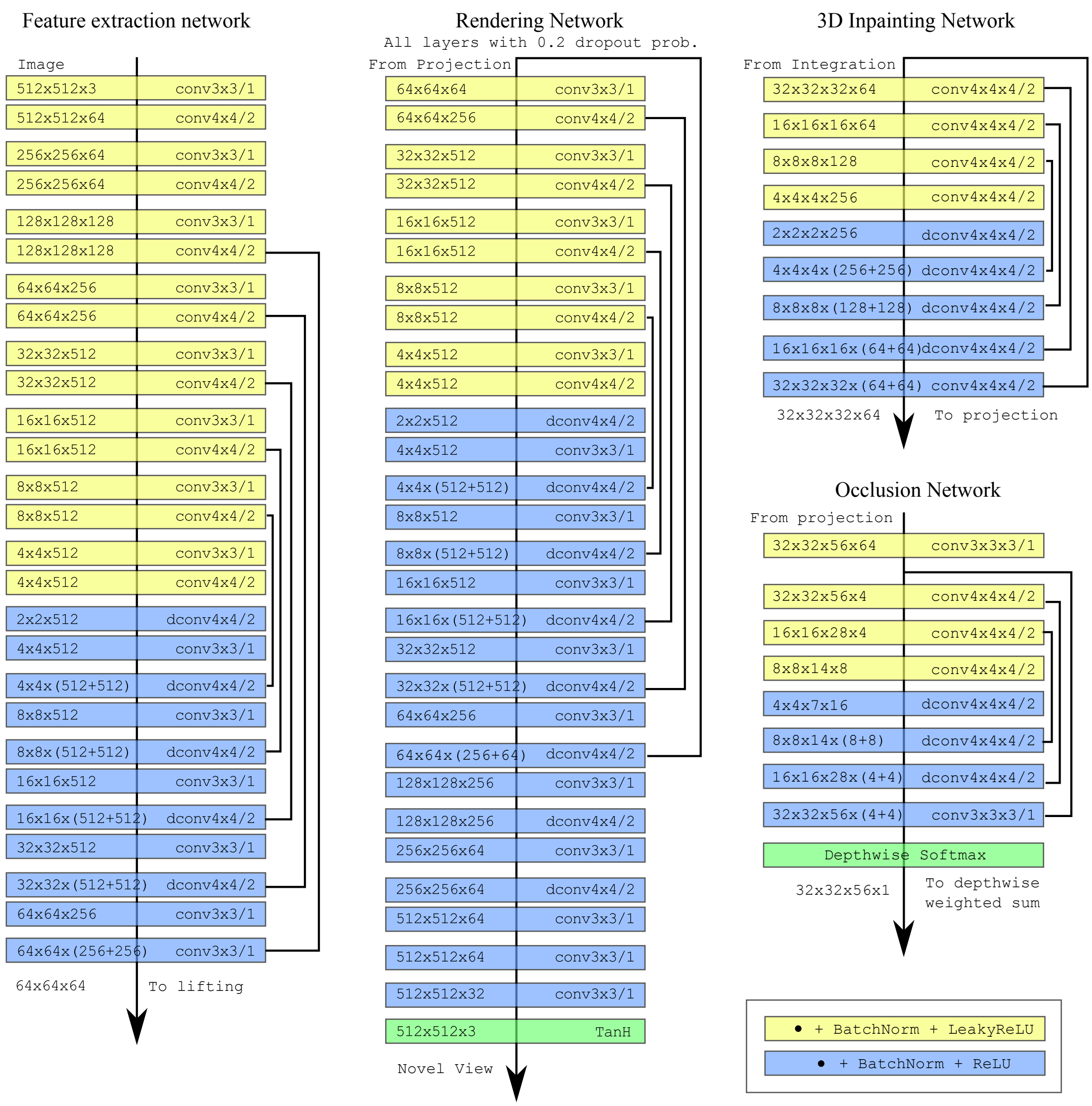

Figure 1: Precise architectures of the feature extraction, rendering, inpainting and occlusion networks. They all follow the basic U-Net structure, while following general best practices in generative network architectures: Reflection padding instead of zero padding, kernel size divisible by stride.

2. Baseline Architecture Tatarchenko et al. [2]

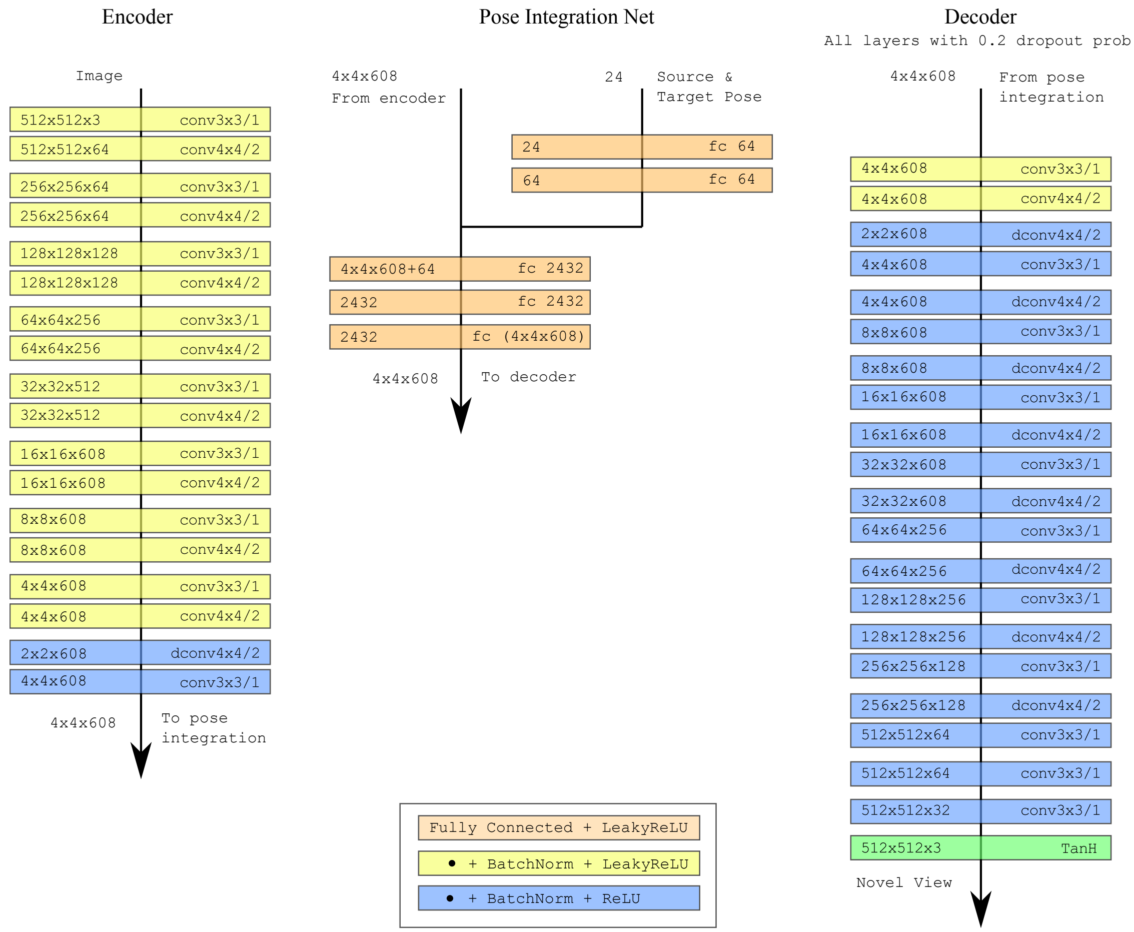

Figure 2: Architectural details of the autoencoder baseline model with latent pose concatenation as proposed by Tatarchenko et al. [2].

3. Baseline Architecture Worrall et al. [3]

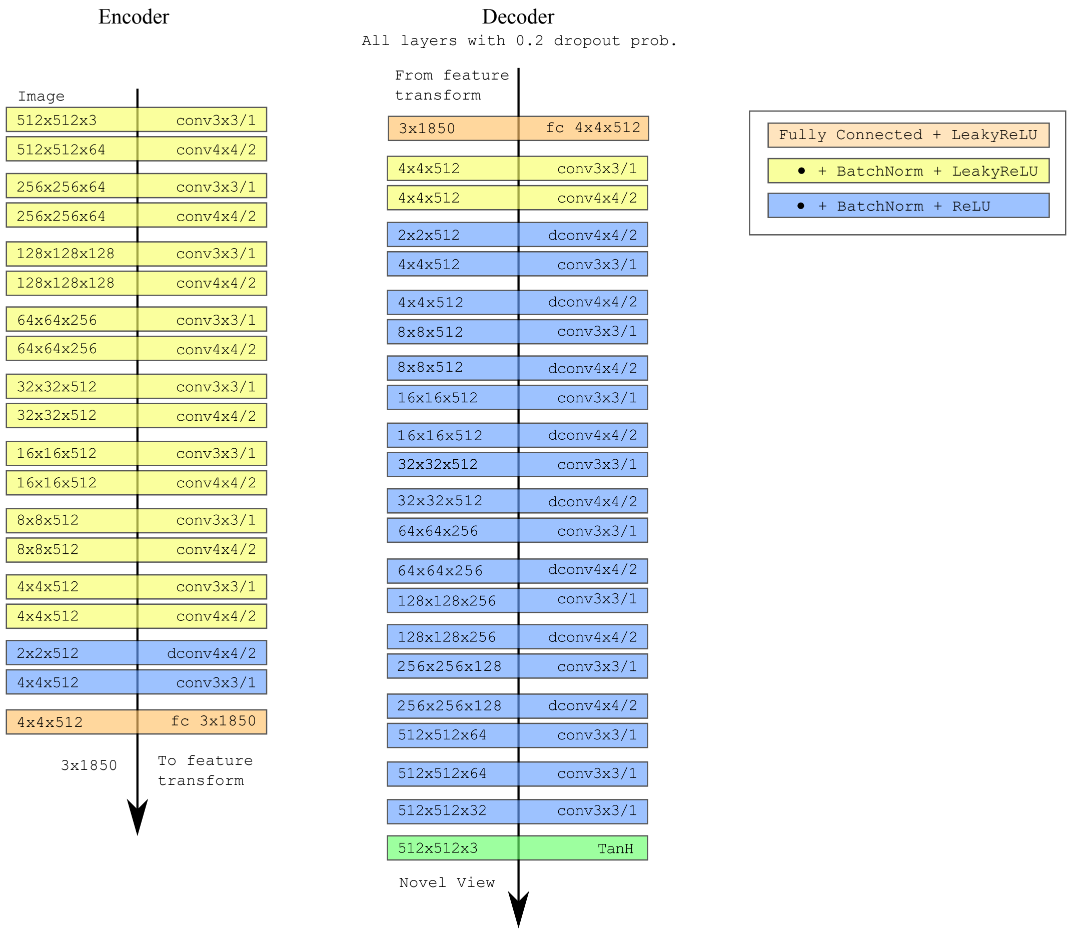

Figure 3: Architectural details of the baseline model based on a rotation-equivariant latent space as proposed by Worrall et al. [3].

4. Baseline Architecture Pix2Pix (Isola et al. [1])

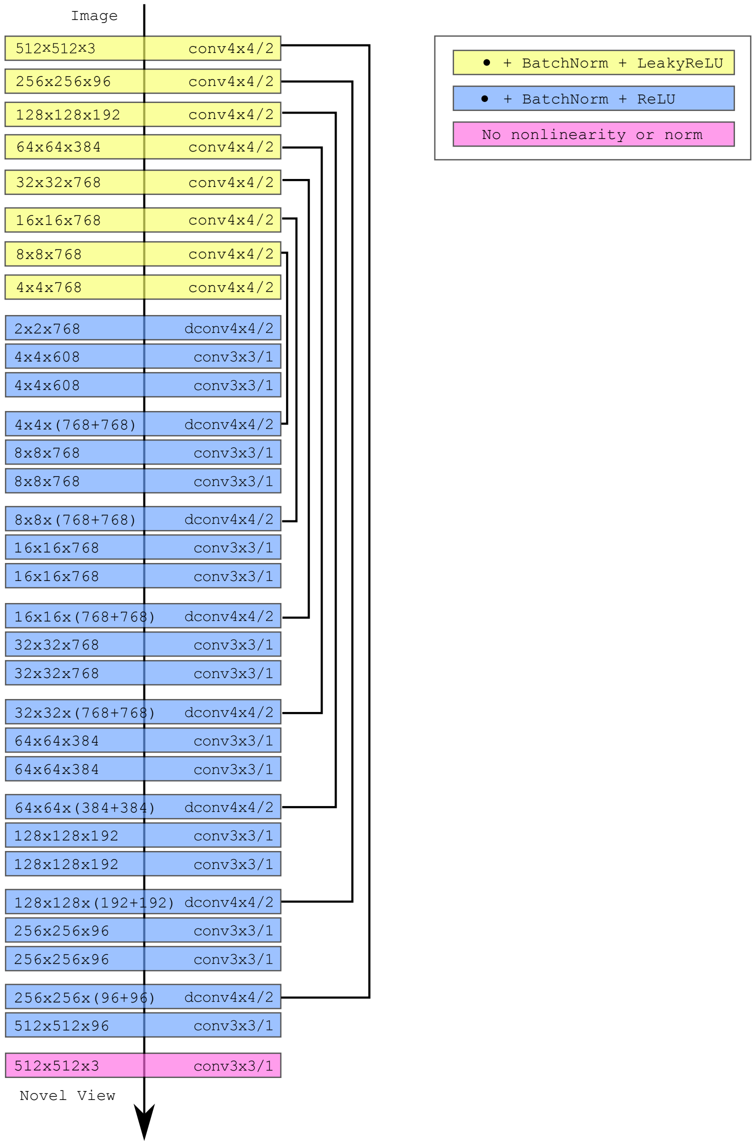

Figure 4: Architectural details of the image-to-image translation baseline model based on Pix2Pix by Isola et al. [1].

5. Comparison of ground-truth depth to estimated depth

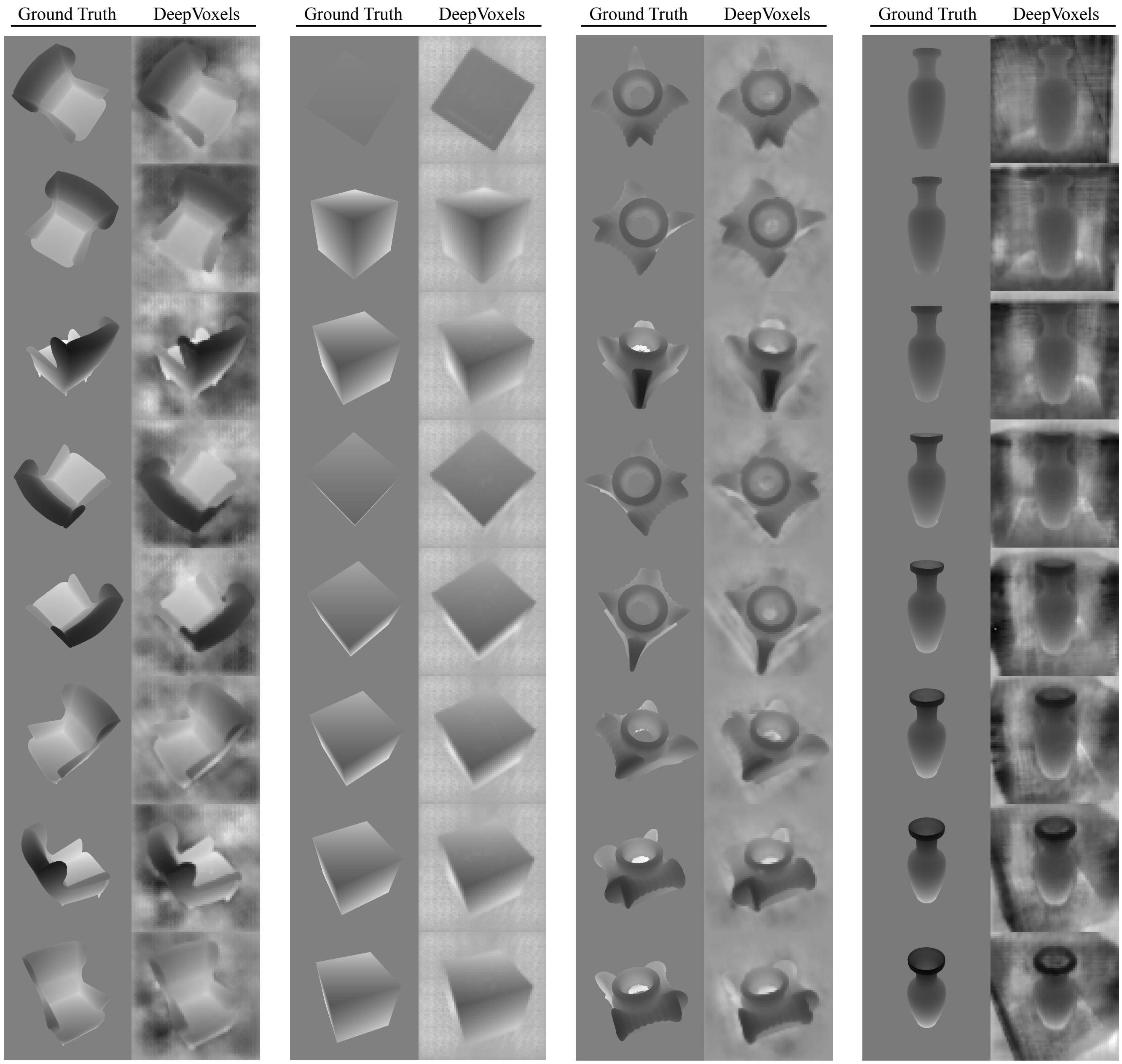

Figure 5: Comparison of ground truth depth maps and the depth maps implicit in the DeepVoxels voxel visibility scores (upsampled from a resolution of 64×64 pixel). We note that these depth maps are learned in a fully unsupervised manner (at no time does our model see a depth map), and only arise out of the necessity to reason about voxel visibility. The background of the depth map is unconstrained in our model, which is why depth values may deviate from ground truth.

6. Pose Extrapolation

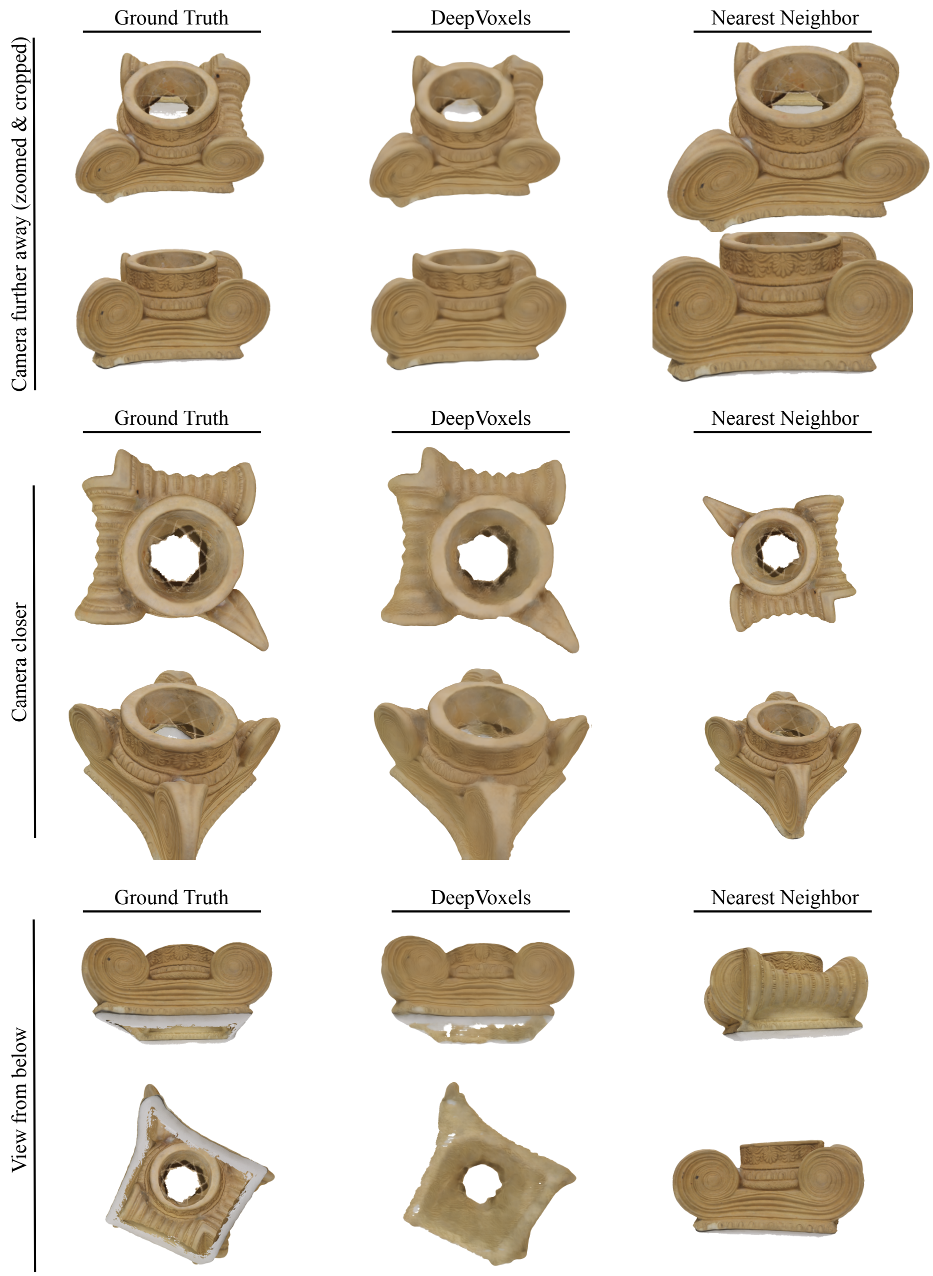

Figure 6: Our training set comprises views sampled at random on the surface of the northern hemisphere. Images in each row are consistently scaled and cropped. We show views that require the model to extrapolate more aggressively - such as increasing the camera distance by a factor of 1.3 (top row), decreasing the camera distance by a factor of 0.75 (middle row) or leaving the northern hemisphere altogether and sampling from the southern hemisphere (bottom row). We show a comparison of ground truth (left column), our model output (center column), and the nearest neighbor in the training set (right column). For the proposed model, detail is lost especially in cases where the model has either never seen these points on the object (bottom row), or where details are seen from closeby for the first time (middle row). Generally, however, the performance degrades gracefully - rigid body motion and general geometry stay consistent, with loss in fine-scale detail and a few failures in occlusion reasoning.

7. Real-World Results

Here, we outline additional details on data captured with a digital single-lens reflex camera as shown in the supplementary video. For this experiment, we captured 457 photographs of a statue. The resolution of each photograph was 1920×1080 pixels. We use sparse bundle adjustment to estimate intrinsic and extrinsic camera parameters. Photographs were subsequently symmetrically center-cropped and downsampled to a resolution of 512×512 pixels. Zoom and focus were set at fixed values throughout the capture. The rest of the processing pipeline is identical to the computer-generated data discussed in the main paper.

References

[1] P. Isola, J.-Y. Zhu, T. Zhou, and A. A. Efros. Image-to-image translation with conditional adversarial networks. In *Proc. CVPR*, pages 5967–5976, 2017. 4

[2] M. Tatarchenko, A. Dosovitskiy, and T. Brox. Single-view to multi-view: Reconstructing unseen views with a convolutional network. *CoRR abs/1511.06702*, 1(2):2, 2015. 2

[3] D. E. Worrall, S. J. Garbin, D. Turmukhambetov, and G. J. Brostow. Interpretable transformations with encoder-decoder networks. In *Proc. ICCV*, volume 4, 2017. 3